Journal of Motor Behavior

ISSN: 0022-2895 (Print) 1940-1027 (Online) Journal homepage: https://www.tandfonline.com/loi/vjmb20

Modular Organization of Exploratory Force Development Under Isometric Conditions in the Human Arm

Jinsook Roh, Sang Wook Lee & Kevin D. Wilger

To cite this article: Jinsook Roh, Sang Wook Lee & Kevin D. Wilger (2019) Modular Organization of Exploratory Force Development Under Isometric Conditions in the Human Arm, Journal of Motor Behavior, 51:1, 83-99, DOI: 10.1080/00222895.2017.1423020

To link to this article: https://doi.org/10.1080/00222895.2017.1423020

Journal of Motor Behavior Vol. 51, No. 1, 2019

RESEARCH ARTICLE

Modular Organization of Exploratory Force Development Under Isometric Conditions in the Human Arm

Jinsook Roh[1,2,3], Sang Wook Lee[4,5,6], Kevin D. Wilger[1,2]

[1]Department of Kinesiology, Temple University, Philadelphia, PA, USA. [2]Neuromotor Science Program, Temple University, Philadelphia, PA, USA. [3]Department of Physical Medicine and Rehabilitation, Feinberg School of Medicine, Northwestern University, Chicago, IL, USA. [4]Department of Biomedical Engineering, Catholic University of America, Washington, DC, USA. [5]Center for Applied Biomechanics and Rehabilitation Research, MedStar National Rehabilitation Hospital, Washington, DC, USA. [6]Human Motor Control Section, National Institute of Neurological Disorders and Stroke, National Institute of Health, Bethesda, MD, USA.

ABSTRACT. Muscle coordination of isometric force production can be explained by a smaller number of modules. Variability in force output, however, is higher during exploratory/transient force development phases than force maintenance phase, and it is not clear whether the same modular structure underlies both phases. In this study, eight neurologically-intact adults isometrically performed target force matches in 54 directions at hands, and electromyographic (EMG) data from eight muscles were parsed into four sequential phases. Despite the varying degree of motor complexity across phases (significant between-phase differences in EMG-force correlation, angular errors, and between-force correlations), the number/composition of motor modules were found equivalent across phases, suggesting that the CNS systematically modulated activation of the same set of motor modules throughout sequential force development.

Keywords: electromyography, force development, motor coordination, motor modules

INTRODUCTION

Humans generate forces with or without the visual feedback on the force to communicate with the external world as activities of daily living, which can look easy to perform but can involve complex calculations to accomplish it. Upper extremity tasks, in many cases, require force production under isometric conditions, such as holding a mug steady while pouring coffee. Isometric reaching is a process in which the arm remains stationary and targeted force output is developed over a transient, exploratory phase. Since isometric reaching is performed with a visual feedback, the mapping between the visual feedback (e.g., displacement of a subject's cursor) and the force characteristics (i.e., direction and amplitude) is required. While isometric reaching in one or two-dimensional (2-D) force space can be generated relatively easy, development of three-dimensional (3-D) targeted forces in an unfamiliar direction requires certain exploration in a subject-specific way. For instance, one may generate isometric reaching at the hand in a lateral-forward-upward direction by producing a directionally tuned force from the beginning of the force generation to match the force target. Others, however, can develop the same target force by sequentially adding each force component to match the force target (e.g., adding lateral force to an initially forward-upward directional force; kinetic redundancy). In addition, force development and maintenance in a targeted direction under a static condition is quite complex from a computational perspective in a mechanically redundant set of muscles. Given a specific force direction, the CNS must appropriately select and activate task-relevant muscles from a highly-redundant arm musculature in order to ramp up and stabilize a proper 3-D force vector at the hand. Furthermore, for typical upper extremity tasks that interact with environment, the direction of an end-point force applied at the hand could largely vary depending on the context of the task, which adds another level of complexity to the motor control. While lower extremity tasks typically require repetitive execution of consistent kinematic patterns and force exertion (i.e., ground reaction force), such as in gait or running, many upper-extremity tasks involve force production toward different directions based on the task requirement (e.g., pushing, pulling, lifting, etc.). Such variation in the task itself could further complicate the selection process of proper muscle coordination patterns performed by the CNS. How the CNS selectively activates arm muscles from a redundant set of muscles (Bernstein, 1967) to develop isometric reaching remains unclear in motor control.

Among various hypotheses examined to resolve the redundancy problem, experimental studies in animal models and humans have suggested that muscle coordination during a given task is performed by modulating the activation of a small number of motor modules, defined here as coordinated activation patterns of a group of muscles (d'Avella, 2003; d'Avella & Lacquaniti, 2013; Dominici et al., 2011; Hart & Giszter, 2004; Lee, 1984; Macpherson, Rushmer, & Dunbar, 1986; Overduin, d'Avella, Roh, & Bizzi, 2008; Torres-Oviedo, Macpherson, & Ting, 2006; Tresch, Saltiel, & Bizzi, 1999). While the motor module paradigm was often employed to explain muscle coordination during repetitive (cyclic) movements that involve spinal pathways (e.g., walking; Clark, Ting, Zajac, Neptune, & Kautz, 2010; Dominici et al., 2011; Monaco, Ghionzoli, & Micera, 2010), the same paradigm was also used to explain complexity in the muscle coordination patterns of

Correspondence address: Jinsook Roh, Department of Kinesiology, Temple University, 1800 N Broad St, Pearson room 268, Philadelphia, PA 19122, USA. e-mail: jinsook.roh@temple.edu

Color versions of one or more of the figures in the article can be found online at www.tandfonline.com/vjmb.

voluntary movements under varying biomechanical conditions (Roh, Rymer, & Beer, 2012) or task conditions, such as voluntary reaching movements toward different target locations (Cheung et al., 2009, 2012; d'Avella, & Lacquaniti, 2013; d'Avella, Fernandez, Portone, & Lacquaniti, 2008; d'Avella, Portone, Fernandez, & Lacquaniti, 2006; Muceli, Boye, d'Avella, & Farina, 2010; Muceli, Falla, & Farina, 2014), hand gestures (Ajiboye & Weir, 2009; Lee, Triandafilou, Lock, & Kamper, 2013), or response to perturbation in different directions (Torres-Oviedo et al., 2006; Torres-Oviedo & Ting, 2007). These studies showed that the human CNS also employs a limited set of motor modules to handle variation in task conditions, such as spatial variation in reaching directions, postural variability, or perturbation directions. However, how humans reach and maintain a stable target force in 3-D force space through an exploratory process at the hand under isometric conditions remains unknown.

While these studies demonstrated that the dimensionality in the "solutions" to the redundancy problem (i.e., muscle coordination patterns of a motor task) was reduced, it did not necessarily substantiate the hypothesis that the modular organization was indeed the mechanism that the CNS employed to obtain these solutions. Motor modules with lower dimensionality may simply result from task constraints and/or the biomechanics of the limb, not resulting from simplified neural control strategies (Kutch, Kuo, Bloch, & Rymer, 2008; Kutch and Valero-Cuevas, 2012; Tresch & Jarc, 2009; Valero-Cuevas, Venkadesan, & Todorov, 2009). For example, previous simulation studies showed that a dimensionality reduction can result from non-neural constraints (Kutch and Valero-Cuevas, 2012). Alternatively, muscle coordination in the redundant musculature might be performed by task constraints and optimizing a performance criterion (De Groote, Jonkers, & Duysens, 2014; Todorov 2004; Todorov & Jordan, 2002). The study using a musculoskeletal model showed that the combination of task constraints and the minimization of muscle effort can explain the low dimensionality of muscle activity recorded during walking (De Groote, Jonkers, & Duysens, 2014). Another study showed that the presence of motor modules decreases the ability of the CNS to vary the properties of the endpoint stiffness and can even preclude the ability to minimize energy (Inouye & Valero-Cuevas, 2016). Particularly, since the tasks examined in the previous studies on the topic of modularity in muscle coordination were frequently-performed daily activities (e.g., reaching movements), the observed reduced dimensionality in the muscle coordination patterns could simply have resulted from an array of "efficient" internal models (inverse/forward; (Wolpert & Ghahramani, 2000) constructed during previous experience.

To test whether the modular organization was indeed employed to construct muscle coordination patterns of reduced dimensionality during force generation, it would be desirable to examine the dimensionality of isometric reaching at different epochs when "naïve" subjects learn to perform relatively new, unfamiliar tasks. We postulate that such an exploratory motor task, isometric reaching in 3-D force space, may involve varying degree of motor complexity across the temporal phases (i.e., during force development), such as significant fluctuations in the correlation between the electromyographic (EMG) and output force. However, we expect that the underlying dimensionality of the muscle coordination would remain unaffected, if activation of motor modules is indeed used to construct multi-muscle coordination patterns.

The purpose of this study was, therefore, to examine the dimensionality during the entire epochs of isometric reaching tasks with a large degree of variation in target locations at the human hand. Note that our previous study (Roh et al., 2012) examined the dimensionality of muscle coordination of the same tasks only during stable force maintenance phase (HOLD). In the current study, we hypothesized that, first, spatiotemporal variability of motor control, quantified by correlations between motor outputs (force components) and correlations between motor output and muscle activation (force-EMG), would be different across different phases of isometric reaching (RAMP1–RAMP3), as the CNS searches for and converges toward a solution (i.e., the muscle coordination of HOLD). However, we also hypothesized that, despite the change in the spatiotemporal variability of motor output, the underlying dimensionality of the muscle coordination during the RAMP phase (i.e., number of motor modules) would remain similar to that of the HOLD phase, if modular organization were indeed employed. A competing hypothesis would be that the CNS does *not* employ modularity during exploratory force development to match a force target under isometric conditions *but* it optimizes certain specific criteria (such as minimum energy) to obtain a motor solution (i.e., matching a force target) during the isometric reaching. In the latter case, the dimensionality of muscle coordination during the RAMP phase would be higher than that of the HOLD phase, reflecting the increased variability in motor output (force). The dataset from this study could be appropriate to test our hypothesis due to its unique experimental design. Unlike the previous studies with typical reaching tasks with 8–16 directional reach targets defined in a 2-D plane (d'Avella et al., 2008; d'Avella et al., 2006; Muceli et al., 2010; Muceli et al., 2014), in this experiment, subjects were instructed to match a set of 54 target force vectors, defined in 3-D space, under an isometric condition. The 3-D force matching task included a relatively larger number of force targets, distributed without a directional bias, many of which would not be used frequently during daily activities and thus would provide a relatively "unfamiliar" sensory feedback. We first analyzed the end-point force exerted during the force RAMP phase,

during which muscle coordination pattern to produce a target force vector was explored and converged to a solution. We also examined whether the muscle coordination during force development could also be explained by the same set of motor modules extracted from the force maintenance phase (HOLD). Additionally, we calculated theoretical solutions for the muscle coordination pattern for the isometric reaching tasks based on an optimization technique that minimizes a cost function (i.e., effort level), and compared its dimensionality (modular structure) with that of experimental data, obtained during different phases (HOLD and RAMP1–RAMP3).

Methods

Participants

Eight young and healthy subjects (3 females; 28.5 ± 3.1 years) participated in the original experiment (Roh et al., 2012). All participants were neurologically intact, and their upper limbs were absent of muscular or orthopedic injuries. The study was performed in accordance with the Declaration of Helsinki, with the approval of the Northwestern University Institutional Review Board. Informed consent was obtained from each subject prior to testing.

Equipment

The experimental task used the Multi-Axis Cartesian-based Arm Rehabilitation Machine (MACARM), a cable-based robot connected to an end effector, a gimbaled handle, described in depth in our previous studies (Roh et al., 2012, 2015; Roh, Rymer, Perreault, Yoo, & Beer, 2013). Each subject grasped the gimbaled handle, mounted on a six-degree-of-freedom (DOF) load cell (Model #45E15A, JR3, Woodland, CA). Forces were sampled at 64 Hz and stored on a computer for subsequent analysis.

Electromyography

Surface EMG data were recorded from eight key arm muscles around the elbow and shoulder joints by using the Bagnoli-8 EMG system (Delsys Incorporated, Boston, MA). Muscles included: brachioradialis (BRD); biceps brachii (BI); triceps brachii, long and lateral heads (TRI_{long} and TRI_{lat}, respectively); deltoid, anterior, medial and posterior fibers (AD, MD, and PD, respectively); and pectoralis major (clavicular fibers; PECTclav). Electrodes were placed in accordance with Hermens et al. (1999) and Perotto, Delagi, and Iazzetti (1980). EMG signals were amplified (× 1000), band-pass filtered (20–450 Hz), and sampled at 1920 Hz.

Experimental Task

The gimbaled handle of the MACARM was placed in a position for the subject's hand to be positioned in front of their ipsilateral shoulder at a distance of 60% of total arm length (Figure 1A). The wrist was braced and trunk was strapped to the chair to prevent motion. A laser pointer was used to monitor changes in a subject's shoulder position, which were verbally corrected if necessary. Prior to data collection, the load cell was re-zeroed to eliminate force signal resulting from posture maintenance and the weight of the limb.

Subjects were given a 2-s baseline period and then 9 s to match a target force. Feedback of the force generated by the subject was displayed on a computer monitor as

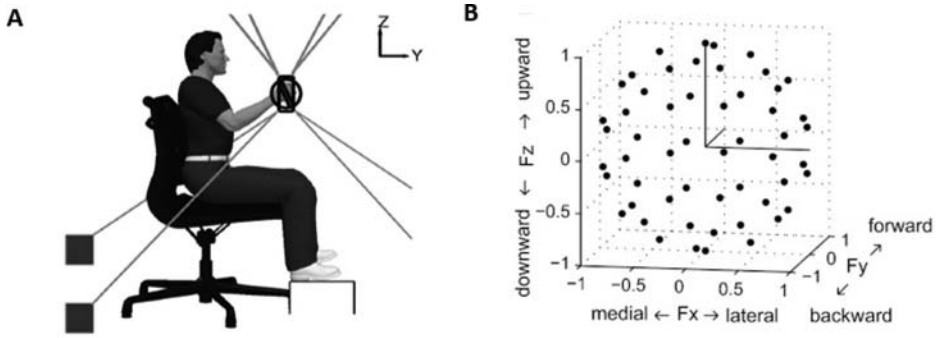

FIGURE 1. Experimental setup and force target directions. A, lateral view of the experimental setup. Multi-Axis Cartesian-based Arm Rehabilitation Machine (MACARM) cable-robot was used to record 3-D forces generated at the hand. The cable-robot includes a spatial array of motors (indicated by black-filled squares) that are connected to a central end-effector via cables (depicted by gray lines). The End-effector includes a gimbaled handle, the bar in the middle of an oval around the subject's right hand in A, mounted on a 6-degree of freedom load cell. Coordinate system for position and force measurements is indicated at top right, and x-axis is out of the paper. B, 54 normalized force targets (black circles) in 3-D force space. To avoid a bias toward any force directions, target force directions were homogeneously distributed in 3-D force space.

a spherical cursor. A successful trial required the subject to match their cursor with a target sphere by ramping up their force and, once in the target zone, holding the force for 1.5 s. The target zone consisted of a sphere with a radius equal to 20% of the targeted force magnitude. Three attempts were permitted before failing a given force target and proceeding to the next random target, but no subjects had a failed target. A 10-s period after each trial and a 1-min rest after each set of 10 trials were provided to minimize fatigue.

Force magnitude was set as 40% of the maximum lateral force (MLF) that the subject could generate with the hand positioned directly in front of the shoulder at a distance of 60% of arm length. Subjects generated voluntary forces in 54 different directions, approximately, uniformly distributed in 3-D force space as shown in Figure 1B. The force components were recorded at 64 Hz. The force direction was presented in a random order. A short training session was provided prior to data collection to ensure that the subject understood the task completely.

EMG Preprocessing

EMGs were preprocessed by subtracting the entire signal mean value, rectified, mean baseline activity subtracted, smoothed with a zero lag fourth-order low pass (20 Hz) Butterworth filter to a linear envelope, and averaged into bins corresponding to a duration of 25 ms. Upon post-hoc visual inspection, an electrocardiographic artifact was found in the PECTclav EMG of two subjects. A wavelet transform was applied to the corrupted raw EMG signal and the high-scale low-frequency components underwent a thresholding process, where coefficients above the threshold were set to zero (Zhou & Kuiken, 2006). The new coefficients were inverse wavelet transformed and preprocessed to obtain the artifact-free EMG. The preprocessed EMG signal was normalized to have unit variance for each muscle to ensure that module extraction would not be biased toward high variance muscles. Prior to module identification, the EMG was parsed into four segments (three epochs of the force development phase and a force maintenance phase): RAMP1, RAMP2, RAMP3, and HOLD. The RAMP1 segment was defined from 70 ms (electromechanical delay; (Aagaard et al., 2002) prior to the onset of end-point force to the beginning of the first 33% of the target magnitude. The onset of end-point force was defined when the force vector magnitude was greater than 2 SD's of the average baseline amplitude. RAMP2 was defined as the period between the beginning of the first 33% and the first 67% of the force target amplitude. Similarly, RAMP3 contained all EMG data from when the end-point force amplitude was the first 67% of the force amplitude to the beginning of the target match. The EMG segments were defined by the onset of force magnitudes and allowed for the force magnitude to go below the onset magnitude. An example of EMG parsing based on force amplitude is denoted as vertical lines in Figure 2A. The number of RAMP segments was also varied ranging from three to five to determine the effect of the number of data segments during RAMP on module identification. HOLD included the EMG activity recorded during the 1.5 s target match interval.

Characterization of Motor Complexity during Force Development

To better quantify the behavioral characteristics of sequential force development, we calculated the relative proportion of the duration of each sub-RAMP period (100%, the entire RAMP duration), as well as the similarity between the directions of the end-point force generated at the hand and its corresponding target force. The duration percentage was calculated by dividing the number of data points in each sub-RAMP by the length of data points in the entire RAMP phase. Both the 3-D end-point force and its associated target force were normalized to a unit vector to calculate the angular deviation between the two 3-D unit vectors in comparison.

In order to quantify the degree of correlation between each muscle activation and the output force amplitude, the correlation coefficient (r^2) was calculated via a linear regression between the force magnitude and each muscle's EMG amplitude. In addition, we calculated the correlation of between-force components (i.e., correlation coefficient (r^2) of Fx–Fy, Fy–Fz, or Fz–Fx; Fx, medialateral, Fy, backward-forward, and Fz, downward-upward directions). The force amplitude of the entire period of force development was divided into that of RAMP1, RAMP2, and RAMP3 periods. Due to the difference in the data acquisition rate (1920 Hz for EMG and 64 Hz for force data), the preprocessed EMG was averaged per force data point to match the length of the force amplitude vector. A One-Way ANOVA on the correlation coefficients of RAMP1, RAMP2, and RAMP3 was calculated, with a post-hoc analysis with Bonferroni correction, whenever required.

Module Identification

A non-negative matrix factorization (NMF) algorithm (Lee & Seung, 2001; 1999) was applied to each EMG dataset to identify motor modules and their activation coefficients. EMG datasets from the RAMP1, RAMP2, RAMP3, and HOLD windows (EMG_{Ramp1}, EMG_{Ramp2}, EMG_{Ramp3}, and EMG_{Hold}) were modeled as a linear combination of a set of N motor modules (W_{Ramp1}, W_{Ramp2}, W_{Ramp3}, and W_{Hold}), respectively, each of which contained a relative level of activation for each of the eight muscles (Cheung et al., 2009, 2012; Cheung, d'Avella, Tresch, & Bizzi, 2005; Hart & Giszter, 2004; Perreault, Chen, Trumbower,

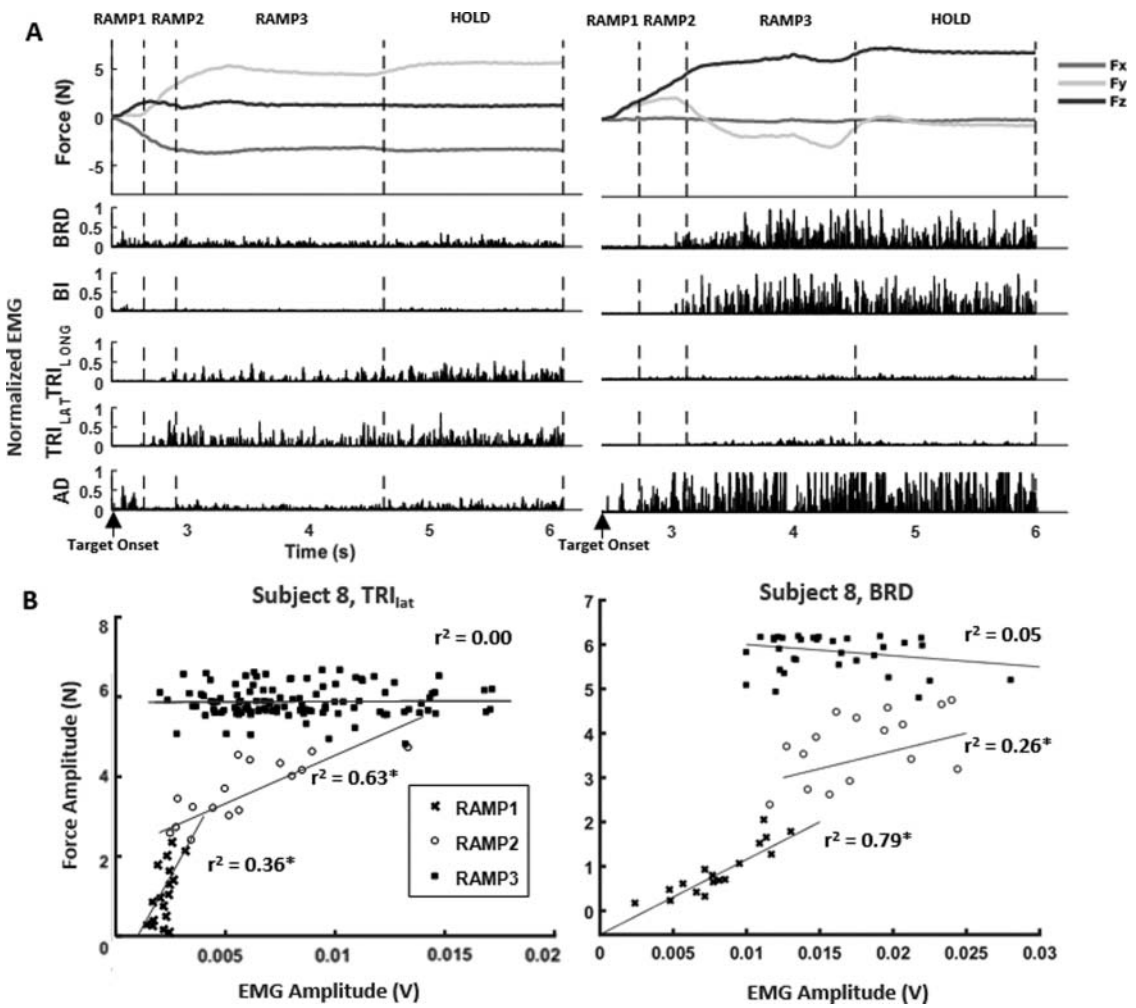

FIGURE 2. Exemplary target matching trials, aligned to the target onset, that show how force and EMG data were parsed into segments and correlation coefficients of muscle activation and output force at the hand, from a representative dataset. A, two exemplary target matching trials. The segmentation of the force and EMG data (depicted by the dotted, vertical lines) was based on the relative proportion of target force magnitude achieved within each trial: (1) RAMP1, from 0 to the beginning of the first 33%, (2) RAMP2, from the first 33% to the beginning of the 67%, (3) RAMP3, from the beginning of the first 67% to the target match (100% amplitude of force target), and (4) HOLD, 1.5 s maintenance of target force. Activation of each muscle was normalized by the maximum value of the muscle activation. Note that the magnitude of the output force components did not linearly scale up during sequential force development phases. B, the correlation coefficients (r^2) of each muscle activation and output force that corresponded to the trials in A. The correlation coefficients (r^2; *, $p < 0.05$) fluctuated across different sequential force development phases for the two exemplary muscles (TRI_{lat} and BRD), the two muscles whose activation magnitude was the largest in the trials depicted as A.

& Lewis, 2008; Roh et al., 2012; Roh, Cheung, & Bizzi, 2011; Torres-Oviedo, Macpherson, & Ting, 2006; Tresch, Cheung, & d'Avella, 2006):

$$\mathrm{EMG}_{\mathrm{Ramp1}}(t) = W_{\mathrm{Ramp1}} \cdot C_{\mathrm{Ramp1}}(t) \quad (1)$$

$$\mathrm{EMG}_{\mathrm{Ramp2}}(t) = W_{\mathrm{Ramp2}} \cdot C_{\mathrm{Ramp2}}(t) \quad (2)$$

$$\mathrm{EMG}_{\mathrm{Ramp3}}(t) = W_{\mathrm{Ramp3}} \cdot C_{\mathrm{Ramp3}}(t) \quad (3)$$

$$\mathrm{EMG}_{\mathrm{Hold}}(t) = W_{\mathrm{Hold}} \cdot C_{\mathrm{Hold}}(t) \quad (4)$$

where W is an $8\times N$ matrix, and the activation coefficient C is an $N \times B$ (number of bins in the dataset) matrix. For each arm, *EMG* was an $8\times B$ matrix, where B was 3240 for the force HOLD dataset (60 bins * 54 trials) and ranged from 307 to 2515 for the RAMP datasets. The number of motor modules in the model, N, was iterated from one to eight and each N had 100 repetitions of the NMF algorithm.

To identify the minimum number of modules that explained the most of the total variance of any EMG dataset, we first calculated variance-accounted-for (VAF) values based on activation of all eight muscles, gVAFs (global VAFs). The total data variation was defined as the trace of the covariance of the EMG-data

matrix, and was used to calculate a multivariate VAF measure:

$$\mathrm{VAF} = 100\mathrm{x}\left(1 - \frac{\mathrm{SSE}}{\mathrm{SST}}\right) \quad (5)$$

where SSE is the summation of the square residuals, and SST was the sum of the squared, uncentered EMG data (Zar, 1999). In addition to the gVAF, we calculated the VAF for each muscle as well as the diffVAF (i.e., difference in gVAF by adding an additional module). The number of modules for each dataset was assessed as the minimum number which met the gVAF >90%, and a diffVAF <3%. This procedure ensured that the estimated number of modules could properly reconstruct the global EMG dataset. Since the initial conditions of motor identification were randomly chosen, module identification procedure was performed with a single dataset 100 times. The repetition that met global criteria was used for the further analysis.

To determine if the dimensionality of muscle activation is conserved across different force developmental phases, a One-Way ANOVA on the mean number of modules per each phase was computed. If a significant difference amongst the four phases was found, a multiple comparison with a Bonferroni correction determined differences between groups.

Module Similarity

A motor module in this study is a mathematical vector whose dimension is the number of the muscles (8) whose activation was recorded. To quantify the similarity between motor modules that underlay RAMP1, RAMP2, and RAMP3 with motor modules that underlay the HOLD period, we took the modules that underlay HOLD as the reference modules and calculated the scalar product of the motor module of any sub-RAMP (any RAMP1–RAMP3) and the reference module in comparison. To determine whether the scalar product between the modules of any sub-RAMP and HOLD periods was larger than that of chance level, we first generated 1000 random modules for both phases. The muscle weights of random modules consisted of random numbers chosen from the uniform distribution. Each random module was normalized to be a unit vector. We then calculated the scalar product of all possible pairs of random modules. The 95th percentile of the distribution of the scalar product was determined to be the cut off for chance level. The similarity of a pair of motor modules in comparison was statistically significant if the scalar product (denoted as *r*-values) was greater than the cut off. We took the modules that underlay HOLD as the reference modules. Per subject, motor modules of each time window (e.g., RAMP1) were compared to the reference modules.

In addition to the scalar product value, the cross-validation gVAF value was calculated to compare motor modules as a group between any sub-RAMP epoch and HOLD, the reference. The cross-validation gVAF was calculated by fitting W_{Ramp1}, W_{Ramp2}, or W_{Ramp3} into $\mathrm{EMG}_{\mathrm{Hold}}$ by multiplying by C_{Hold} and vice versa for the HOLD dataset. In addition to examining whether the cross-validation met the gVAF criteria, a One-Way ANOVA was computed between the average gVAF of the four conditions (RAMP into RAMP, HOLD into RAMP, RAMP into HOLD, HOLD into HOLD) to determine differences in cross-validation gVAF between the RAMP and HOLD modules.

Module Activation and its Tuning Direction

To observe changes in the recruitment (or activation) of modules across RAMP1, RAMP2, RAMP3, and HOLD, the activation coefficients of motor modules were averaged per trial. A One-Way ANOVA was computed to find any difference amongst the averaged activation coefficient across RAMP1, RAMP2, RAMP3, and HOLD. If a significant difference was found, a multiple comparison of groups (Bonferroni correction) determined which force developmental phases were statistically different.

In addition to the magnitude of its activation coefficient, the preferred direction of each module activation was assessed. The force targets were scaled by each module's activation and summed. The unit vector of the summation was defined as the tuning vector for the module activation, or the preferred direction. We then calculated the angular deviation of each phase's preferred direction to the average of the preferred directions across the four phases (RAMP1–RAMP3 and HOLD). To establish a chance level threshold for the angle between the preferred direction of motor module at each phase and the direction averaged across the four phases, we first generated 1000 random 3-D unit vectors. Second, we calculated the angular deviation between the random unit vectors and each average direction. The fifth percentile of the angle distribution (alpha = 0.05) was the threshold for similarity.

Simulation of Muscle Activation Pattern using Optimization Technique

We also computed activation patterns of the eight muscles for the target tasks using an optimization technique in order to obtain theoretical solutions that minimize energy expenditure, which represents our competing hypothesis. We extracted motor modules from the simulated muscle coordination patterns using the same computational procedure described above, and compared the number and modular structure of two patterns (theoretical vs. experimental) to examine whether this alternative theoretical model could explain the observed dimensionality of muscle coordination during isometric reaching tasks.

We first constructed a biomechanical model of the upper extremity musculoskeletal system by utilizing anatomical data of subjects (i.e., segment length) and their posture during task, as well as moment arm and cross-sectional area data of the eight muscles obtained from the literature (Holzbaur, Murray, & Delp, 2005). The endpoint force was then computed from the Jacobian and joint moments produced by activating the eight muscles, and the cost function was defined as a weighted sum of the effort and task error, similar to those reported in previous studies (e.g., Emken, Benitez, Sideris, Bobrow, & Reinkensmeyer, 2007). A constrained nonlinear optimization technique was implemented to obtain activation level of the eight muscles in MATLAB environment (MathWorks Inc., Natick, MA) (fmincon function). We extracted motor modules from the obtained muscle coordination pattern, following the same procedure described above, which represents the dimensionality of the theoretical solution of muscle coordination based on minimum energy expenditure.

Results

Spatiotemporal Characteristics of Isometric Reaching Vary Across Different Epochs of Force Development

As shown in the representative trial (Figure 2A), most subjects adopted a strategy to rapidly increase the force amplitude initially, up to about 70% of the target force magnitude (represented as RAMP1 and RAMP2), then to deliberately fine-tune the direction of the force vector as they approached the target force magnitude (RAMP3). Since the output force did not linearly ramp up during the exploratory isometric reaching, the correlation coefficient between each muscle activity (e.g. TRI_{lat} or BRD) and output force was different across sequential sub-RAMP epochs (Figure 2B; *, $p < 0.05$). The observed difference in the temporal duration of the three ramp phases (Figure 3A) indicates that subjects spent significantly longer time on the final phase of the ramp (RAMP3; ANOVA, $F_{(2,21)} = 43.75$, $p < 0.001$) during which the force magnitude increased from 67% to 100% of the target force across subjects ($n = 8$). The directional error between the target and produced force vectors, quantified by the angle between the two vectors, was also found to improve significantly over the course of force development across subjects (ANOVA, $F_{(2,21)} = 82.88$, $p < 0.001$; $n = 8$; Figure 3B).

The correlation between the force components (Fx–Fy, Fx–Fz, Fy–Fz) also contrasted different motor control strategies used during the early force development phases (RAMP1 and RAMP2) and during the late phase (RAMP3; Figure 3C). For the force pairs in the transverse plane (Fx–Fy), sagittal plane (Fy–Fz), and coronal plane (Fx–Fz), there was a significant decrease in the between-force correlation (r^2 values) in the last ramp phase across subjects (RAMP3; for Fx–Fy, $F_{(2,21)} = 31.60$, $p < 0.0001$; for

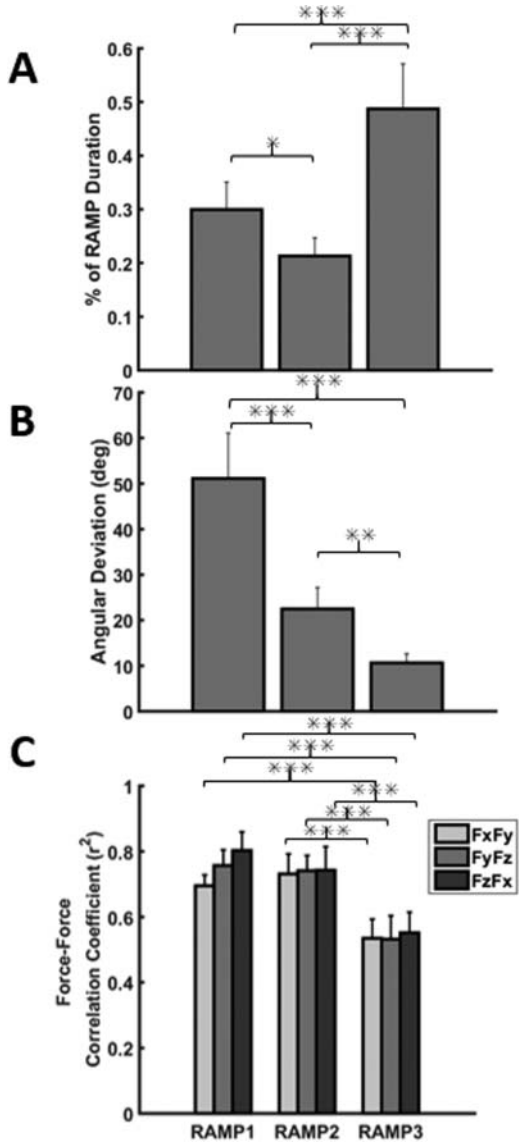

FIGURE 3. Spatiotemporal characteristics of force development across subjects ($n = 8$; mean ± SD). A, the relative durations of the force development spent at early, middle, and later phases of RAMP (RAMP1–RAMP3), respectively, across all force targets. The relative duration of sub-RAMP phases was significantly different from each other (*, $p < 0.05$; ***, $p < 0.001$). B, the angular deviation of the output force from a given target force direction. The angular deviation of each sub-phase decreased across sequential force development and was different from each other (**, $p < 0.01$; ***, $p < 0.001$). C, the correlation coefficient (r^2) of between-force components (e.g., r^2 of Fx and Fy; ***, $p < 0.001$). Note that subjects initially increased the force magnitude rather rapidly, then started "fine-tuning" the output force direction during the last phase of the force development to match the target. Note also that the motor complexity, indicated by between-force correlations, was different between earlier and later phases of force development (RAMP1 and RAMP2 vs. RAMP3).

Fy–Fz, $F_{(2,21)} = 39.31$, $p < 0.0001$; for Fz–Fx, $F_{(2,21)} = 33.33$, $p < 0.0001$; $n = 8$), indicating decoupled control of these force components. Similar between-phase differences (RAMP1 and RAMP2 vs. RAMP3) were observed in the correlation between individual muscle activation and the force magnitude (Figure 2B), which indicated that the correlations between EMG-output force decreased as the target force developed (all p-values < 0.05).

The Number and Composition of Motor Modules Required to Predict Muscle Activation Patterns was Similar Across Different Epochs of Force Development

Given any number of motor modules (1–8), the degree of variance in the muscle coordination explained by these modules were not significantly different across the different epochs of force development (ANOVA, $F_{(3,28)} = 0.22$, $p = 0.8831$; $n = 8$; Figure 4A). As the number of motor modules increased, the portion of the total variance explained by the motor modules (gVAF) increased, as expected. With four modules, on average, 94.41 ± 1.85; 94.14 ± 1.65; 94.40 ± 1.57; and 94.59 ± 1.32% of gVAF were accounted for at RAMP1–RAMP3 and HOLD, respectively ($n = 8$). The result indicates that the complexity of the EMG data did not change in the sequential force development at the human hand.

Across the different phases of force development, three to five motor modules were identified to predict EMG patterns of each subject (Figure 4B), given the criteria to estimate the appropriate number of modules (see Methods). On average, four modules were identified at each of the four phases (3.75 ± 1.04; 3.88 ± 0.83; 3.50 ± 0.76; and 3.63 ± 0.52, mean ± SD; $n = 8$ subjects). At RAMP1 and RAMP2, except for one subject, the EMG data of most subjects required three to five modules. Most subjects (five out of eight) required three and four modules at RAMP3 and HOLD, respectively. However, the number of modules identified from the four phases (RAMP1–RAMP3 and HOLD) was not statistically different (ANOVA, $F_{(3,28)} = 0.32$, $p = 0.8111$). Any minute changes in the criteria applied to identify the appropriate number of modules (e.g. the diffVAF from 3% to 5%) did not change the results.

The composition of motor modules activated during the initial, middle, and final phase of force development as well as stable target force production appears conserved. Each of the four motor modules consisted of muscle weights illustrated as the distribution of the weights superimposed to their mean value (Figure 5A; $n = 8$ subjects; demarcated as the black box). While "elbow flexor (E Flex)" was dominated by the activation of BRD and BI (two elbow flexors), "elbow extensor (E Ext)" typically involved activation of TRI_{long} and TRI_{lat} (two elbow extensors). The third module, "shoulder adductor/flexor (S Add/Flex)," consisted of BI, AD, MD, and PECTclav. The fourth one, "shoulder abductor/extensor (S Abd/Ext)," typically included the activation of MD, PD, and two or three elbow muscles.

The similarity index (r-values), indicating the similarity of the individual module vector of sub-RAMP phases and the corresponding one of HOLD, shows that the motor modules of the sequential force development and stable force maintenance are similar ($n = 8$; mean ± SD). The r-values, indicated at the right corner of each module of RAMP, were over the chance level (chance level = 0.9186; $p < 0.05$) at all sub-RAMP phases except for three values during the initial phase of force development. During RAMP1, two out of eight subjects' data had low signal-to-noise ratio (SNR) in the EMG data. If these datasets with low SNR were omitted from the analysis, the r-values of the remaining subjects' data were 0.95 ± 0.03 (for E Flex), 0.91 ± 0.07 (for E Ext), and 0.92 ± 0.07 (for S Abd/Ext),

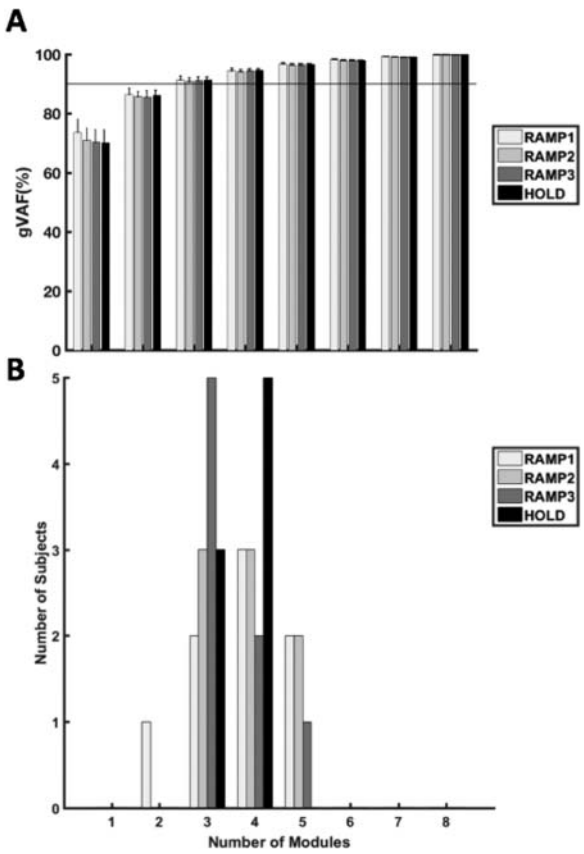

FIGURE 4. Typically, three to five motor modules predicted the muscle activation patterns of isometric force developmental phases in the human arm. A, global variance-accounted for (gVAF) as a function of the number of motor modules used for EMG prediction ($n = 8$; mean ± SD). B, histogram that shows the number of motor modules required to predict EMGs underlying 3-D isometric force development and maintenance of target force (RAMP1–RAMP3 and HOLD, respectively). Typically, four modules were required for all four groups, accounting for, on average, 94.4% of total variance of EMGs in each group.

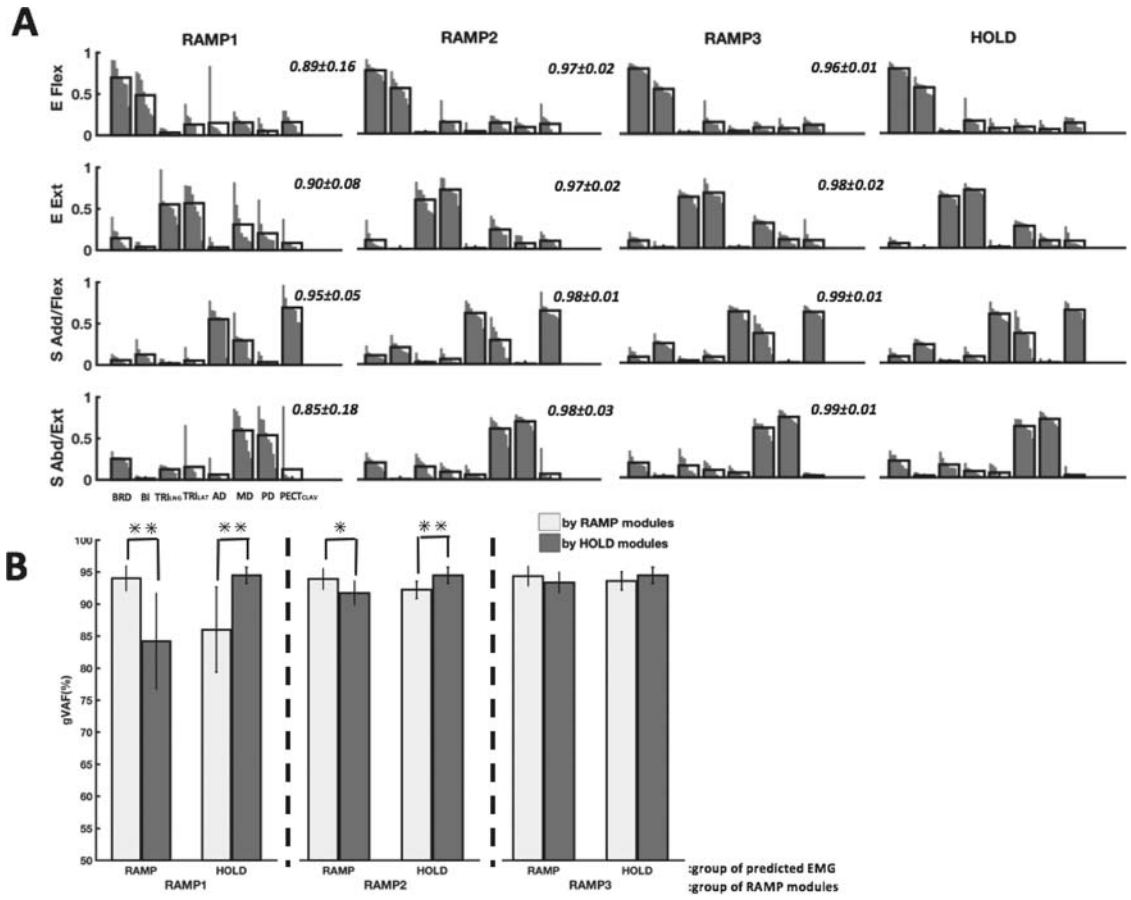

FIGURE 5. Comparison of motor modules identified from different phases of force development. A, four motor modules identified from EMGs recorded during each phase of sequential isometric reaching and target force maintenance. The modules are labeled according to the mechanical action of the main muscles activated within each module: elbow flexor (E Flex), elbow extensor (E Ext), shoulder adductor/flexor (S Add/Flex), and shoulder abductor/extensor (S Abd/Ext) modules. For each module, the muscle weights (y-axis) as the group mean ($n = 8$) are superimposed on the distribution of the corresponding muscle weights. The r-value next to each motor module indicates the scalar products between the module of sub-RAMP and its corresponding module of HOLD ($n = 8$; mean $\pm$ SD). Most r-values were statistically significant (t-test, $p < 0.05$). B, cross-validation VAF values by comparing motor modules of each epoch (ex. RAMP1, etc) of isometric reaching to motor modules of HOLD period as a group. Note that the all cross-validation VAF values were high, over 84%, though the VAF values of earlier RAMP period (RAMP1 or RAMP2) and HOLD period were statistically different (*, $p < 0.05$; **, $p < 0.01$). Overall, the results indicate that motor modules activated during stable force generation (HOLD) were also activated during different epochs of isometric reaching.

statistically significant, respectively ($p < 0.05$; in all cases, $n = 8$, mean $\pm$ SD).

The cross-validation gVAF values also show that the motor modules activated during different epochs of isometric reaching are comparably similar to the modules of force maintenance (Figure 5B). Though the gVAF values were statistically different (**, $p < 0.01$) by comparing RAMP1 to HOLD, the values were already high (over 84%). Note that, due to the lower EMG amplitude recorded during the earlier phases of RAMP, the structure of resultant motor modules could be affected by random noise simultaneously recorded with the EMG signals. The cross-validation VAF values were not statistically different by comparing the data between the later epoch of isometric reaching (RAMP3) and HOLD ($p > 0.05$).

Activation Coefficients of Motor Modules are Task-specifically Modulated to Achieve Force Target Matches

The modulation of the activation coefficients of motor modules was target force-specific over the course of isometric reaching. Depending on the direction of target forces, certain modules, identified from the EMG of RAMP1–RAMP3 and HOLD, were activated more than the rest (Figure 6A). Typically, more than two motor modules were activated at each sub-phase of force development per target. For example, while E Flex and S Add/Flex modules

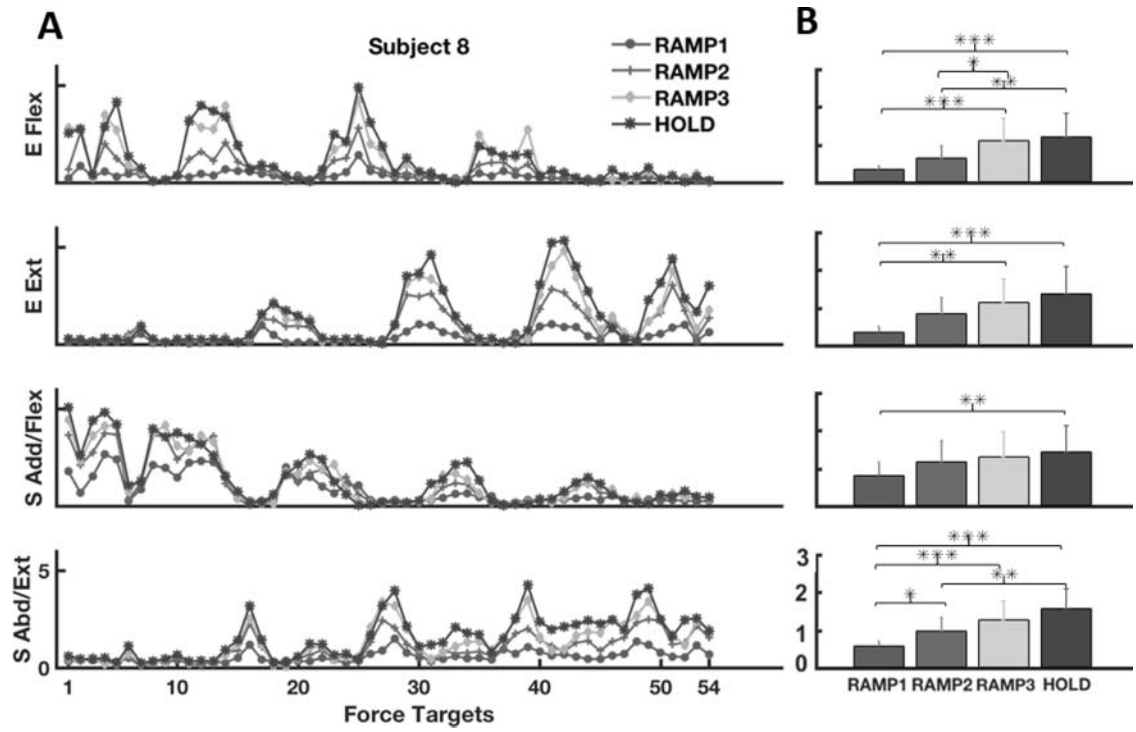

FIGURE 6. The activation coefficient of motor modules is modulated to meet task requirements. A, the averaged activation coefficients of four motor modules displayed as a function of 54 force targets at each force development phase in *Subject 8*. B, multiple comparison of the magnitude of the activation coefficients at three sub-RAMP and HOLD periods (*, $p < 0.05$; **, $p < 0.01$; ***, $p < 0.001$).

were activated during the development of the fifth target force, the activation coefficients of E Ext and S Abd/Ext were less. Despite the non-linear increase in the end-point force magnitude (Figure 2A) and the fluctuation of task performance (Figures 2B, 3B, and 3C) over sequential force development, the activation coefficients of motor modules were systematically modulated to underlie the force development trajectory, which was observed across all individual datasets.

The mean ($n = 54$ targets) of activation coefficients of motor modules increased as end-point force developed per subject (Figure 6B). Across all four modules for a representative subject in Figure 6B, the mean recruitment of motor module was different between the early phase of force development and stable force maintenance phase (RAMP1 and HOLD; $p < 0.01$), which was the same for all subjects ($n = 8$). The modulation of the activation coefficients of four motor modules predicted the segmental EMGs well. For example, for each EMG segment recorded from a representative subject (*Subject 8*), over 86% of the total variance of each original EMG channel data (colored in black) at each force development phase was explained by the activation of the four motor modules (the four bottom panels), except for BI of RAMP1 (Figure 7). The relatively low VAF value of BI at RAMP1 was due to the low amplitude of the activation of the muscle. Once the amplitude of the muscle activation became larger at RAMP2–RAMP3 and HOLD, the four modules could reconstruct the EMG of the same muscle to over 87%. The tendency was the same for the rest of subjects' data. Based on the activation of the four modules, on average, 76.89 ± 18.93%, 82.29 ± 11.00%, 84.53 ± 7.05%, and 85.12 ± 6.52% of muscle VAF was accounted for in the RAMP1, RAMP2, RAMP3, and HOLD, respectively ($n = 8$; mean ± SD). These results suggest that the development of 3-D forces under isometric conditions in the human arm is mediated by modulating the activation coefficients of the same motor modules from the beginning of force generation.

The Tuning Directions of Modules in Force Space and Across Subjects

The tuning direction of module activation was relatively similar across different phases of force development. Figure 8 shows that the tuning direction of each module's activation coefficient in the two 2-D force plots in a representative subject (*Subject 8*). Across all subjects, the length of the mean vector was 508.81 ± 49.62, 550.12 ±

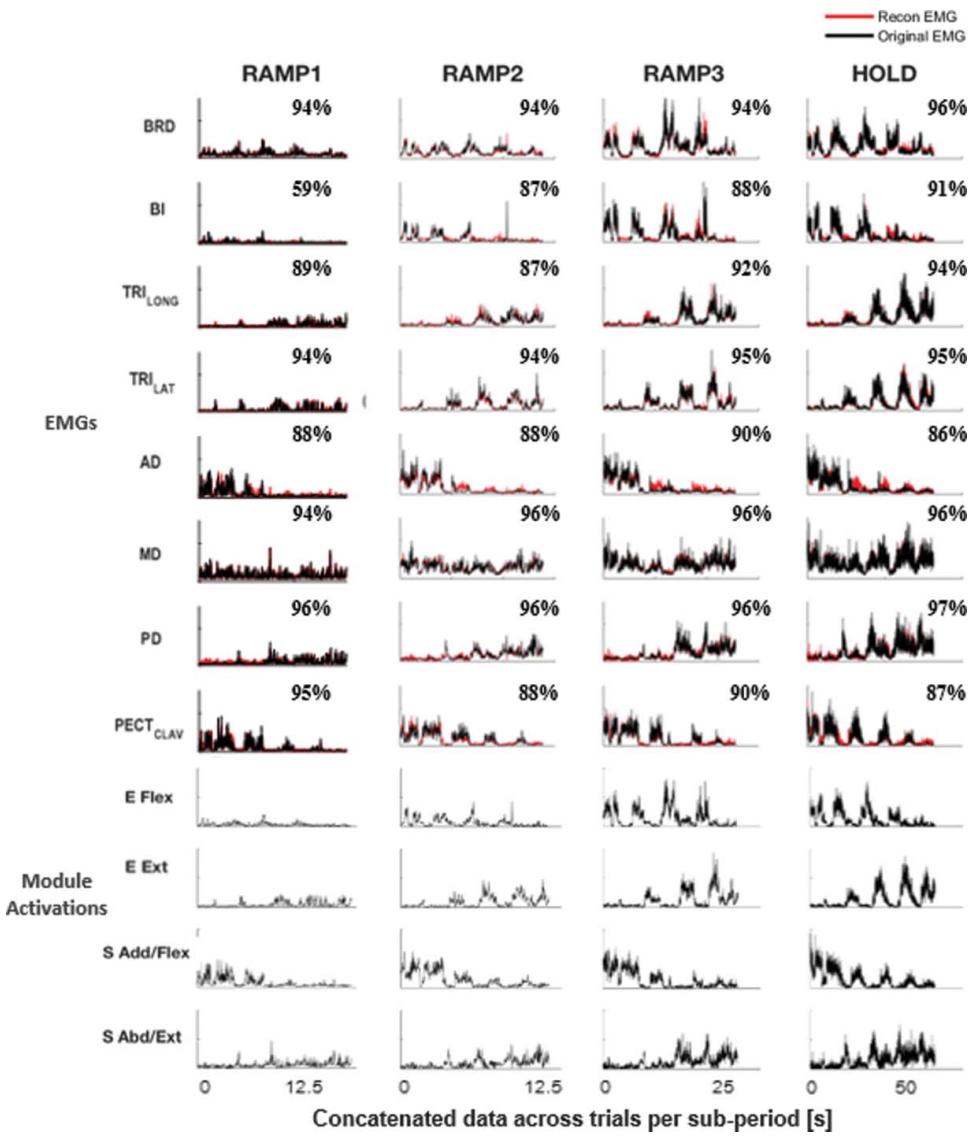

FIGURE 7. The original (black) and reconstructed (red) EMG data, recorded from eight muscles during RAMP1-RAMP3 and HOLD periods, are concatenated across 54 associated force targets. The EMG data are followed by the activation coefficients of four motor modules for a typical subject (*Subject 8*).

74.85, 571.82 ± 64.92, and 479.91 ± 61.23 for each module, respectively ($n = 8$; mean ± SD). The angular deviation among the mean of the four time windows' tuning directions and each of the four directions was not different for three out of four modules ($p < 0.05$; E Ext, S Add/Flex, and S Abd/Ext) and different for E Flex. Across all subjects, the mean angular deviations for the four motor modules were 11.22 ± 6.06, 9.80 ± 5.13, 8.58 ± 3.77, and 8.23 ± 5.40 degrees, respectively ($n = 8$; mean ± SD), which were statistically smaller than the chance level ($p < 0.05$). In addition to the similarity of motor modules as individual modules and as a group (Figures 5A and 5B, respectively), this small, angular deviation of tuning directions supports that modular representation of isometric force development is relatively similar across subjects.

Optimization-based Solutions of Muscle Coordination Showed Higher Dimensionality than Experimental Data

The dimensionality of the simulated EMG data, obtained by implementing the optimization criteria that minimized effort level and task error, was larger than that of the experimental data, when the same criteria (see Methods) were applied to determine the appropriate number of motor modules (Figure 9). On average, the larger number (five) of motor modules were required to explain the optimization-

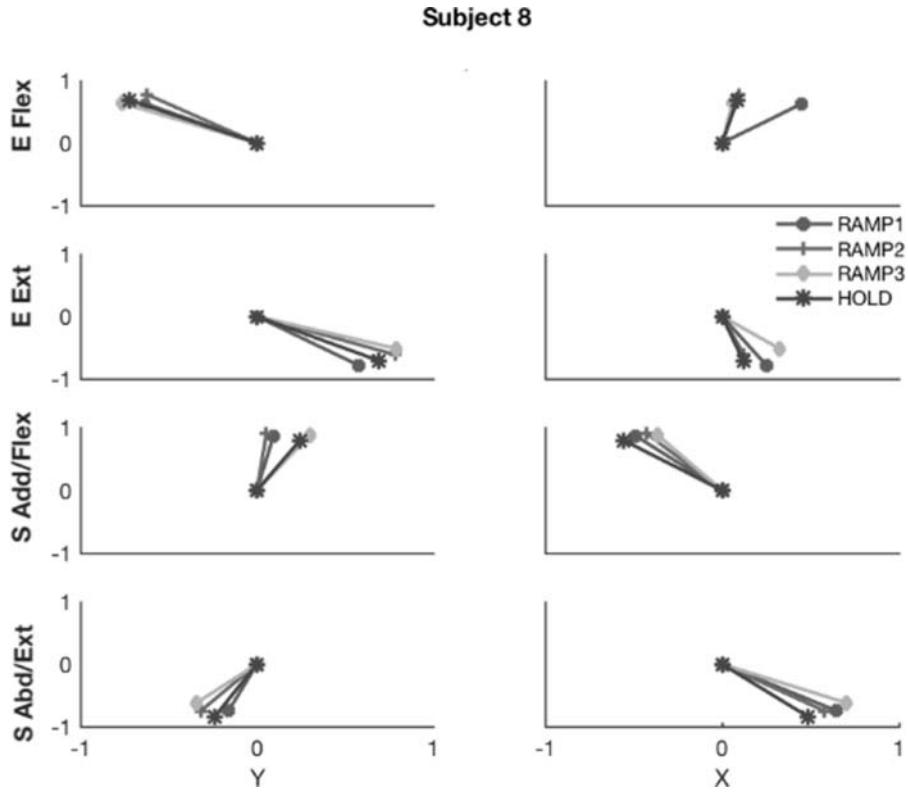

FIGURE 8. Tuning vectors of motor module activations as unit vectors in the four conditions (RAMP1–RAMP3 and HOLD) in the 3-D force space (Z-directional force presented in y-axis). The angular deviation between the mean of the four phases' tuning directions and the four directions corresponding to the four time windows was not different for three out of four modules (E Ext, S Add/Flex, and S Abd/Ext).

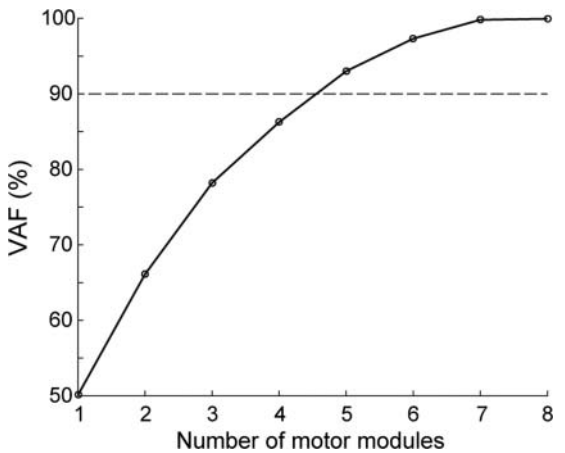

FIGURE 9. The variance-accounted for (VAF) as a function of the number of motor modules used for the prediction of the simulated EMG data. The dimensionality of the optimization-based EMG pattern, simulated by minimizing effort level and task error, was five, on average, which was larger than that of the experimental data.

based muscle coordination patterns obtained for the varying force magnitudes.

Discussion

The primary goal of this study was to examine how multi-muscle activation is coordinated over the course of exploratory isometric reaching, a motor task to develop a target force output toward a range of 3-D target locations when the arm remains stationary, especially from the perspective of modularity. The spatiotemporal characteristics of the force profile appeared to vary across the sequential phases, indicated by the varying EMG-force relationship within each episode of isometric reaching as well as the varying relative duration and angular errors in force direction of different epochs of force development. The data suggest that, during the exploratory isometric reaching, the output force amplitude did not linearly ramp up, and the correlation between each muscle activity and output force decreased nonlinearly. During the force development, people attempted to increase magnitude of the output force at earlier phases, while allowing relatively large error in the direction. Then the strategy switched toward fine-tuning the

direction of end-point force to match the target force vector as the force magnitude became similar to the target. In addition, the exploratory isometric reaching was characterized by the significant decrease in the angular deviation from the target force direction and between-force correlations, indicating fine tuning of the force direction. Despite the varying level of motor complexity across the different phases, the dimensionality and composition of muscle coordination during force development was conserved (i.e., the number and composition of the motor modules were consistent across the phases). Our results support that the CNS activates the same set of motor modules for sequential, exploratory force development under isometric conditions.

Comparison with the Previous studies in Muscle Coordination of Static Force Generation

The selection of muscle coordination patterns to produce isometric submaximal forces have been studied in the human upper extremity, for example, in the task of force generation at the fingertip (Valero-Cuevas, 2000), precision grip (Maier & Heppreymond, 1995), and force target matching at the hand (Berger & d'Avella, 2014; Borzelli, Berger, Pai, & d'Avella, 2013; Roh et al., 2012), etc. Though some studies addressed the modularity or synergistic nature of muscle coordination, the coordination characteristics of different epochs of isometric reaching procedure remain unclear (Berger & d'Avella 2014; Borzelli et al., 2013; Roh et al., 2012). For instance, the synergistic relationship of muscle activation was calculated based on pairwise correlation (Maier & Heppreymond, 1995), which, in turn, cannot elucidate an overarching neural strategy that underlies the observed coordinated control of multiple muscles. Some studies qualitatively characterized different phases of force generation, but did not identify motor modules or their dimensionality during the task (Valero-Cuevas, 2000). As an extension of the previous study (Roh et al., 2012), the current study aimed to examine, from the modular control perspective, how humans coordinate multi-muscle activation during exploratory, sequential isometric force development toward a range of directions in 3-D force space at the hand.

Modular Organization of Muscle Coordination During Force Development

Examination of the experimental data suggests that the force development in the current experiment can be divided into phases of different control strategies (e.g., feedforward vs. feedback). In our study, most target tasks were rather unfamiliar to subjects, as the target location was randomly chosen out of 54 targets equally distributed in 3-D force space and none of these tasks was repeated more than three times. The amplitude of output force components and EMG-force relationship did not linearly scale up or down during different epochs of isometric reaching (Figure 2). As indicated by the duration of different ramp phases (Figure 3A), most subjects appeared to initially increase the force magnitude toward the target direction rather rapidly (up to RAMP2: 67% of the target force magnitude), then started "fine-tuning" the force direction during the last phase of the force development based on the visual feedback (RAMP3). Note that the force direction during initial force development (RAMP1) was not directed precisely toward the target direction (Figure 3B). Therefore, it appears that, when exposed to a novel force production task, subjects initially "executed" the task roughly based upon the given task goal (feedforward control), then at the later phase, they incorporate visual feedback information to "fine-tune" and meet the task requirement. This finding is consistent with previous studies that suggested "serial corrections" during task, based upon sensory feedback information, are performed continuously (Doeringer & Hogan, 1998; Gawthrop, Loram, Lakie, & Gollee, 2011; Loram & Lakie, 2002).

Despite the different nature of these phases (RAMP1, RAMP2 vs. RAMP3 vs. HOLD), interestingly, the dimensionality/complexity of the multi-muscle coordination did *not* significantly vary across these phases; the number of motor modules extracted from any phase of the task performance was not significantly different from the other phases (4 modules across all 54 direction), which indicates that the complexity of the neural process that produced (seemingly-complex) time-varying muscle coordination patterns, observed during "fine-tuning" phase (RAMP3), was essentially the same level with the simple force maintenance phase (HOLD). Furthermore, the detailed analysis of the motor module composition also revealed that the motor modules employed during these different epochs of isometric reaching were essentially identical (see below), providing strong support for a modular control architecture for force development under isometric conditions.

Comparisons of Motor Modules Underlying Different Epochs of Isometric Reaching

The similarity analyses on motor modules revealed that the dimensionality of motor control during isometric reaching and force maintenance tasks can be reduced to a strikingly simple level; for most subjects, only three to five modules were found to be required in order to reconstruct muscle coordination used for isometric reaching toward 54 different directions (Figure 4B). Previous studies suggested that, for the control of reaching movement, the CNS may initially use an internal model to construct an open-loop controller, while online correction during movements (based upon sensory feedback) may be performed by modulating motor module coefficients (d'Avella, & Lacquaniti, 2013; d'Avella, Portone, & Lacquaniti, 2011) in the later phase. Our results support this notion – note that only a small number of motor modules were required to reconstruct muscle coordination patterns used during the "fine-

tuning" phase (RAMP3), during which individual muscle activation does *not* seem to be correlated with the task (correlation coefficient). Furthermore, it appears that the same modules used in the initial execution (RAMP1 and 2) were used in the later exploration phase (RAMP3), supporting the notion that the same motor modules initially selected by an "open-loop" controller (e.g., internal model; (Kalaska, Scott, Cisek, & Sergio, 1997) are used throughout the fine-tuning phase (RAMP3) and maintenance (HOLD), which would greatly simplify the control of complex motor task (force development toward a large number of 3-D target locations).

Previous studies on finger force generation also showed that when modulating fingertip force magnitude across the voluntary range, the number of contributing muscles and the relative activity among them was not changed (Valero-Cuevas, 2000). Though this study did not identify motor modules underlying the fingertip force, its results also suggest that the development of sub-maximal target force is simplified by scaling the magnitude of intermuscular coordination patterns. Note that the task complexity of this previous study (production of "well-defined" three orthogonal end-point forces) was much lower than our current study (exploratory force production toward 54 different directions defined in 3-D force space), which may explain why the correlation between the endpoint force and muscle activation level remained very high throughout the entire force production in their data – such "well-defined" tasks would not have necessitated the feedback control observed in the later phase (RAMP3) of our study. We still reason that our results are congruent with the findings from this study to some degree, as the results from both studies demonstrate that the CNS adopts simplified neural strategies to resolve redundancy in the musculoskeletal system.

A Case for Modular Organization of Muscle Coordination

Our results support the notion that a limited number of motor modules are employed to develop and maintain a large range of 3-D force vectors. While each task performance could be divided into phases of different nature (feedforward vs. feedback), the complexity of motor control during these phases remained approximately the same throughout the task. Note that, if the coordination of multiple muscles were not mediated by the modular structure, one would expect to see increased variability/dimensionality of the muscle coordination patterns during feedback control (e.g., Baweja, Patel, Martinkewiz, Vu, & Christou, 2009). Although variability in the individual muscle activation during the "fine-tuning" phase of the force production (RAMP3) was much higher, the structural variability (the number of motor module) remained the same, which strongly supports the notion of modular organization of isometric force production. It should also be acknowledged that a higher number of motor modules were extracted from the muscle activation patterns simulated from an optimization (minimum effort) across different phases of force development, which also supports this notion of modular organization. However, caution should also be exercised to interpret this simulation results, as the change in the simulation parameters and musculoskeletal model could have resulted in different muscle coordination patterns with different modular structure. In addition, the current experiment did not test all directions and magnitudes of force (the entire feasible force set), which should have been tested to conclusively attribute the identified synergy structure to the nervous system (Kutch and Valero-Cuevas 2012).

It should be acknowledged that, considering the high dimensionality of the target task (54 directions), the use of a limited number of modules (three to four) could also have resulted in "biomechanically-inefficient" solutions (i.e., non-optimal muscle coordination) in many cases (Figure 9); note that each of the eight muscles observed in this study possesses distinct biomechanical function (except for the TRI_{long} and TRI_{lat} muscles), and given the nature of the variability presented in the target task (equally dividing the entire possible workspace of the 3-D force vector into 54 different directions), a larger number of modules should have been employed to achieve "optimal" solutions across different force directions (e.g., minimum-energy or minimum-force solutions). Therefore, it is plausible that, facing high complexity of the motor task, the CNS may have simplified the neural control at the expense of biomechanical efficiency.

Methodological Considerations

Though the number of motor modules identified from the EMG of the initial phase of force development (RAMP1) was comparable to that identified at the later phases of force development, the mean ($n = 8$ subjects) r-values of three motor modules at RAMP1 appeared lower than the chance level due to the EMG data of two out of eight subjects (Figure 5A). In addition, the cross-validation VAF based on the activation of four motor modules at RAMP1 to reconstruct the EMG of stable force production (HOLD) was lower than that of the other phases (Figure 5B). We reason that the results are due to the low signal-to-noise level of the EMG collected at RAMP1 corresponding to the low force amplitude subjects generated from zero force. The result remains a limitation to interpret whether humans used a larger repertoire of motor modules at the beginning of force development and reduced the number to match a target force. So, we identified to what extent the extra module could account for the total variance of the EMG data of RAMP1, which was found typically less than 1.94% across subjects ($n = 8$). Also, the activation of the extra module was not tuned to any specific force space, suggesting that the role of the module activation in specific force generation was not clear. Thus, we rather identified the same number of motor modules from each segmental data and compared the composition and activation of the modules to

examine the characteristics of modularity in sequential, isometric force development.

A potential cross-talk amongst the surface EMG electrodes placed over the arm muscles may be conceivable as a factor that can affect the composition of motor modules. Previous studies showed that the composition of motor modules identified from the activities of muscles during human reaching, some of which we collected for the current study, was not significantly altered even though the muscles mostly affected by potential cross-talk were eliminated from the analyses (d'Avella et al., 20062008). Prior to further data analyses, we also visually inspected that the EMG response of each muscle was different from each other within each trial. We reason that these results suggest that the effects of potential cross-talk on the modularity of the EMG data were minimal in the study.

The number of data segments during RAMP was operationally defined (early, middle, and later phases of force development in terms of the portion of a target force amplitude). To avoid any methodology-specific description of a given EMG dataset, we tested the effects of the segment number on the modularity by varying the number of RAMP segments from three to five. The number of data segments did not affect the primary characteristics of modularity in muscle coordination in the sense that the number and composition of the modules are relatively conserved and the recruitment of each module scales up during the sequential isometric reaching.

Since it took a different duration of time for each subject to ramp up one's end-point force to match a given target, the number of data points of RAMP periods was different across subjects. In addition, the typical duration of RAMP (1.31 ± 0.25 s; $n = 8$) was different from that of HOLD period (1 s). To test the effects of a different duration of periods in comparison in motor module analysis, *ad hoc* analyses were performed with the matched number of RAMP and HOLD data points of the same subject and between different subjects by randomly selecting the data points from the data of a longer period. The inherent mismatch between the numbers of RAMP and HOLD periods within and across subjects did not affect the main findings of the study.

Conclusion

This study aimed to examine the characteristics of multi-muscle coordination underlying an exploratory, isometric reaching, and force maintenance task. While a relatively rapid increase in the force amplitude was dominant at the earlier phases of force development, the main objective was shifted toward the fine-tuning of the force direction to match a given force target at the later phase of force generation. The varying level of motor complexity across the phases was also indicated by the variation in the correlation of muscle activation and output force and between-force correlations. However, the same set of motor modules were found to underlie the muscle coordination patterns employed during the different phases. Our results support the idea that the CNS recruits and activates a limited number of motor modules to meet a variety of task goals.

ACKNOWLEDGMENTS

The authors wish to thank Randall F. Beer and William Z. Rymer for the support of data collection and Seng Bum Yoo for assistance with data collection.

FUNDING

The research reported in this publication was supported by the American Heart Association (17SDG33670561; and PI, J. Roh).

REFERENCES

Aagaard, P., Simonsen, E. B., Andersen, J. L., Magnusson, P., & Dyhre-Poulsen, P. (2002). Increased rate of force development and neural drive of human skeletal muscle following resistance training. *Journal of Applied Physiology*, *93*(4), 1318–1326. doi:10.1152/japplphysiol.00283.2002.

Ajiboye, A. B., & Weir, R. F. (2009). Muscle synergies as a predictive framework for the EMG patterns of new hand postures. *Journal of Neural Engineering*, *6*(3). doi:10.1088/1741-2560/6/3/036004.

Baweja, H. S., Patel, B. K., Martinkewiz, J. D., Vu, J., & Christou, E. A. (2009). Removal of visual feedback alters muscle activity and reduces force variability during constant isometric contractions. *Experimental Brain Research*, *197*, 35–47. doi:10.1007/s00221-009-1883-5.

Berger DJ, & d'Avella A. (2014). Effective force control by muscle synergies. *Frontiers in Computational Neuroscience*, *8*, 46. doi:10.3389/fncom.2014.00046.

Bernstein, N. (1967). *The co-ordination and regulation of movements*. Oxford: Pergamon.

Borzelli, D., Berger, D. J., Pai, D. K., & d'Avella, A. (2013). Effort minimization and synergistic muscle recruitment for three-dimensional force generation. *Frontiers in Computational Neuroscience*, *7*, 186. doi:10.3389/fncom.2013.00186.

Cheung, V. C. K., d'Avella, A., Tresch, M. C., & Bizzi, E. (2005). Central and sensory contributions to the activation and organization of muscle synergies during natural motor behaviors. *Journal of Neuroscience*, *25*, 6419–6434. doi:10.1523/JNEUROSCI.4904-04.2005.

Cheung, V. C. K., Piron, L., Agostini, M., Silvoni, S., Turolla, A., & Bizzi, E. (2009). Stability of muscle synergies for voluntary actions after cortical stroke in humans. *Proceedings of the National Academy of Sciences of the United States of America*, *106*, 19563–19568. doi:10.1073/pnas.0910114106.

Cheung, V. C. K., Turolla, A., Agostini, M., Silvoni, S., Bennis, C., Kasi, P., … Bizzi, E. (2012). Muscle synergy patterns as physiological markers of motor cortical damage. *Proceedings of the National Academy of Sciences of the United States of America*, *109*, 14652–14656. doi:10.1073/pnas.1212056109.

Clark, D. J., Ting, L. H., Zajac, F. E., Neptune, R. R., & Kautz, S. A. (2010). Merging of healthy motor modules predicts reduced locomotor performance and muscle coordination complexity post-stroke. *Journal of Neurophysiology*, *103*, 844–857. doi:10.1152/jn.00825.2009.

d'Avella, A., Saltiel, P., & Bizzi, E. (2003). Combinations of muscle synergies in the construction of a natural motor behavior. *Nature Neuroscience*, *6*(3), 300–308. doi:10.1038/Nn1010.

d'Avella, A., Fernandez, L., Portone, A., & Lacquaniti, F. (2008). Modulation of phasic and tonic muscle synergies with reaching direction and speed. *Journal of Neurophysiology*, *100*, 1433–1454. doi:10.1152/jn.01377.2007.

d'Avella, A., & Lacquaniti, F. (2013). Control of reaching movements by muscle synergy combinations. *Frontiers in Computational Neuroscience*, *7*, 42. doi:10.3389/fncom.2013.00042.

d'Avella, A., Portone, A., Fernandez, L., & Lacquaniti, F. (2006). Control of fast-reaching movements by muscle synergy combinations. *Journal of Neuroscience*, *26*, 7791–7810. doi:10.1523/JNEUROSCI.0830-06.2006.

d'Avella, A., Portone, A, & Lacquaniti, F. (2011). Superposition and modulation of muscle synergies for reaching in response to a change in target location. *Journal of Neurophysiology*, *106*, 2796–2812. doi:10.1152/jn.00675.2010.

De Groote, F., Jonkers, I., & Duysens, J. (2014). Task constraints and minimization of muscle effort result in a small number of muscle synergies during gait. *Frontiers in Computational Neuroscience*, *8*, 115. doi:10.3389/fncom.2014.00115.

Doeringer, J. A., & Hogan, N. (1998). Intermittency in preplanned elbow movements persists in the absence of visual feedback. *Journal of Neurophysiology*, *80*, 1787–1799. doi:10.1152/jn.1998.80.4.1787.

Dominici, N., Ivanenko, Y. P., Cappellini, G., d'Avella, A., Mondi, V., Cicchese, M., . . . Lacquaniti, F. (2011). Locomotor primitives in newborn babies and their development. *Science*, *334*, 997–999. doi:10.1126/science.1210617.

Emken, J. L., Benitez, R., Sideris, A., Bobrow, J. E., & Reinkensmeyer, D. J. (2007). Motor adaptation as a greedy optimization of error and effort. *Journal of Neurophysiology*, *97*, 3997–4006. doi:10.1152/jn.01095.2006.

Gawthrop, P., Loram, I., Lakie, M., & Gollee, H. (2011). Intermittent control: A computational theory of human control. *Biological Cybernetics*, *104*, 31–51. doi:10.1007/s00422-010-0416-4.

Hart, C. B., & Giszter, S. F. (2004). Modular premotor drives and unit bursts as primitives for frog motor behaviors. *Journal of Neuroscience*, *24*, 5269–5282. doi:10.1523/JNEUROSCI.5626-03.2004.

Hermens, H., Freriks, B., Merletti, R., Stegeman, D., Blok, J., Rau, G., . . . Hagg, G. (1999). *European recommendations for surface electromyography, results of the SENIAM Project*. Netherlands: Roessingh Research and Development.

Holzbaur, K. R. S., Murray, W. M., & Delp, S. L. (2005). A model of the upper extremity for simulating musculoskeletal surgery and analyzing neuromuscular control. *Annals of Biomedical Engineering*, *33*, 829–840. doi:10.1007/s10439-005-3320-7.

Inouye, J. M., & Valero-Cuevas, F. J. (2016). Muscle synergies heavily influence the neural control of arm endpoint stiffness and energy consumption. *PLoS Computational Biology*, *12*, E1004737. doi:10.1371/journal.pcbi.1004737.

Kalaska, J. F., Scott, S. H., Cisek, P., & Sergio, L. E. (1997). Cortical control of reaching movements. *Current Opinion in Neurobiology*, *7*, 849–859. doi:10.1016/S0959-4388(97)80146-8.

Kutch, J. J., Kuo, A. D., Bloch, A. M., & Rymer, W. Z. (2008). Endpoint force fluctuations reveal flexible rather than synergistic patterns of muscle cooperation. *Journal of Neurophysiology*, *100*, 2455–2471. doi:10.1152/jn.90274.2008.

Kutch, J. J., & Valero-Cuevas F. J. (2012). Challenges and new approaches to proving the existence of muscle synergies of neural origin. *PLOS Computational Biology*, *8*, e1002434. doi:10.1371/journal.pcbi.1002434.

Lee, D. D., & Seung, H. S. (2001). Algorithms for non-negative matrix factorization. In Todd. K. Leen, Thomas G. Dietterich, & Volker Tresp (Eds.), *Advances in neural information processing systems 13* (pp. 556–562).

Lee, D. D., & Seung, H. S. (1999). Learning the parts of objects by non-negative matrix factorization. *Nature*, *401*, 788–791. doi:10.1038/44565.

Lee, S. W., Triandafilou, K., Lock, B. A., & Kamper, D. G. (2013). Impairment in task-specific modulation of muscle coordination correlates with the severity of hand impairment following stroke. *Plos One*, *8*(7), e68745. doi:10.1371/journal.pone.0068745.

Lee, W. A. (1984). Neuromotor synergies as a basis for coordinated intentional action. *Journal of Motor Behavior*, *16*: 135–170. doi:10.1080/00222895.1984.10735316.

Loram, I. D., & Lakie, M. (2002). Human balancing of an inverted pendulum: Position control by small, ballistic-like, throw and catch movements. *The Journal of Physiology*, *540*, 1111–1124. doi:10.1113/jphysiol.2001.013077.

Macpherson, J. M., Rushmer, D. S., & Dunbar, D. C. (1986). Postural responses in the cat to unexpected rotations of the supporting surface – evidence for a centrally generated synergic organization. *Experimental Brain Research*, *62*, 152–160. doi:10.1007/BF00237411.

Maier, M. A., & Heppreymond, M. C. (1995). EMG activation patterns during force production in precision grip. 2. Muscular synergies in the spatial and temporal domain. *Experimental Brain Research*, *103*, 123–136. doi:10.1007/BF00241970.

Monaco, V., Ghionzoli, A., & Micera, S. (2010). Age-related modifications of muscle synergies and spinal cord activity during locomotion. *Journal of Neurophysiology*, *104*, 2092–2102. doi:10.1152/jn.00525.2009.

Muceli, S., Boye, A. T., d'Avella, A., & Farina, D. (2010). Identifying representative synergy matrices for describing muscular activation patterns during multidirectional reaching in the horizontal plane. *Journal of Neurophysiology*, *103*, 1532–1542. doi:10.1152/jn.00559.2009.

Muceli, S., Falla, D., & Farina, D. (2014). Reorganization of muscle synergies during multidirectional reaching in the horizontal plane with experimental muscle pain. *Journal of Neurophysiology*, *111*, 1615–1630. doi:10.1152/jn.00147.2013.

Overduin, S. A., d'Avella, A., Roh, J., & Bizzi, E. (2008). Modulation of muscle synergy recruitment in primate grasping. *Journal of Neuroscience*, *28*, 880–892. doi:10.1523/JNEUROSCI.2869-07.2008.

Perotto, A., Delagi, E., & Iazzetti, J. (1980). *Anatomical guide for the electromyographer: The limbs and trunk*. Springfield, IL: Charles C. Thomas.

Perreault, E. J., Chen, K., Trumbower, R. D., & Lewis, G. (2008). Interactions with compliant loads alter stretch reflex gains but not intermuscular coordination. *Journal of Neurophysiology*, *99*, 2101–2113. doi:10.1152/jn.01094.2007.

Roh, J., Cheung, V. C. K., & Bizzi, E. (2011). Modules in the brain stem and spinal cord underlying motor behaviors. *Journal of Neurophysiology*, *106*, 1363–1378. doi:10.1152/jn.00842.2010.

Roh, J., Rymer, W. Z., & Beer, R. F. (2012). Robustness of muscle synergies underlying three-dimensional force generation at the hand in healthy humans. *Journal of Neurophysiology*, *107*, 2123–2142. doi:10.1152/jn.00173.2011.

Roh, J., Rymer, W. Z., & Beer, R. F. (2015). Evidence for altered upper extremity muscle synergies in chronic stroke survivors with mild and moderate impairment. *Frontiers in Human Neuroscience*, *9*, 6. doi:10.3389/fnhum.2015.00006.

Roh, J., Rymer, W. Z., Perreault, E. J., Yoo, S. B., & Beer, R. F. (2013). Alterations in upper limb muscle synergy structure in chronic stroke survivors. *Journal of Neurophysiology*, *109*, 768–781. doi:10.1152/jn.00670.2012.

Todorov E. (2004). Optimality principles in sensorimotor control. *Nature Neuroscience*, *7*, 907–915. doi:10.1038/nn1309.

Todorov, E., & Jordan, M. I. (2002). Optimal feedback control as a theory of motor coordination. *Nature Neuroscience*, *5*, 1226–1235. doi:10.1038/nn963.

Torres-Oviedo, G., Macpherson, J. M., & Ting, L. H. (2006). Muscle synergy organization is robust across a variety of postural perturbations. *Journal of Neurophysiology*, *96*, 1530–1546. doi:10.1152/jn.00810.2005.

Torres-Oviedo, G., & Ting, L. H. (2007). Muscle synergies characterizing human postural responses. *Journal of Neurophysiology*, *98*, 2144–2156. doi:10.1152/jn.01360.2006.

Tresch, M. C., Cheung, V. C. K., & d'Avella, A. (2006). Matrix factorization algorithms for the identification of muscle synergies: Evaluation on simulated and experimental data sets. *Journal of Neurophysiology*, *95*, 2199–2212. doi:10.1152/jn.00222.2005.

Tresch, M. C., & Jarc, A. (2009). The case for and against muscle synergies. *Current Opinion in Neurobiology*, *19*, 601–607. doi:10.1016/j.conb.2009.09.002.

Tresch, M. C., Saltiel, P., & Bizzi, E. (1999). The construction of movement by the spinal cord. *Nature Neuroscience*, *2*, 162–167. doi:10.1038/5721.

Valero-Cuevas, F. J. (2000). Predictive modulation of muscle coordination pattern magnitude scales fingertip force magnitude over the voluntary range. *Journal of Neurophysiology*, *83*, 1469–1479. doi:10.1152/jn.2000.83.3.1469.

Valero-Cuevas, F. J., Venkadesan, M., & Todorov, E. (2009). Structured variability of muscle activations supports the minimal intervention principle of motor control. *Journal of Neurophysiology*, *102*, 59–68. doi:10.1152/jn.90324.2008.

Wolpert, D. M., & Ghahramani, Z. (2000). Computational principles of movement neuroscience. *Nature Neuroscience*, *3* Suppl, 1212–1217, doi:10.1038/81497.

Zar, J. (1999). *Biostatistical analysis*. Upper Saddle River, NJ: Prentice-Hall.

Zhou, P., & Kuiken, T. A. (2006). Eliminating cardiac contamination from myoelectric control signals developed by targeted muscle reinnervation. *Physiological Measurement*, *27*, 1311–1327. doi:10.1088/0967-3334/27/12/005.

Received March 19, 2017
Revised November 6, 2017
Accepted December 15, 2017